

Modeling of the Kinetics of Confined Nonwetting Flow in a Mesoporous Particle

Y. Qiao* and X. Kong

Department of Civil Engineering, University of Akron, Akron, OH 44329-3905, USA

Received March 4, 2004; revised version received April 21, 2004; accepted July 15, 2004

PACS numbers: 05.20.Dd; 05.20.Jj; 47.60.+i

Abstract

In this paper a quantitative model of the confined flow in a mesoporous particle has been developed. The particle is initially surrounded by a nonwetting liquid. As the external pressure increases to the critical value such that the capillary effect is overcome, the liquid is forced into the mesopores. The confined inflow in the three-dimensional mesoporous environment is modeled as the effective phase transformation involving nucleation, growth, and coalescence of filled mesopore clusters. The influences of the pore size distribution and the external pressure are analyzed.

1. Introduction

Since the last century a number of synthetic mesoporous materials have been developed, especially in the past two decades [1]. They are of important relevance to sensing, catalysis, dielectric coating, and molecular sieve applications and have been widely applied in the areas of environmental, biotechnological, and chemical engineering. One of the most suitable network materials is silica. Through the well established synergistic co-assembly method, in which the silica network and the template are first formed simultaneously and then the template is removed by liquid-liquid extraction [2, 3], nearly homogeneous and isotropic mesoporous silica particles with various surface properties can be obtained [4]. The pore size is usually in the range of 2–80 nm, leading to the high specific area around 200–2000 m²/g, which is the most dominant characteristic. In the interior of the particle the three-dimensional interpenetrating porous structure can be considered as a nanovoid-surrounding network covalently crosslinked together, as depicted in Fig. 1 [5]. Usually, the particle size ranges from 1 micron to 1 mm.

In applications of catalysis or selective absorption, as well as characterization procedures such as mercury porosimetry, the mesoporous particles are often immersed in non-wetting liquids such as polymer melts/solutions and, if the particles are hydrophobic, water. The external pressure, p , can vary in a large range. If p is smaller than the critical value, p_{cr} , the solid phase and the liquid phase are separate due to the capillary effect, while if $p > p_{cr}$ the nonwetting liquid can be forced into the mesopores (see Fig. 2). The behaviors of the confined inflow, particularly the inflow rate v and the saturation time t_s , are critical to the precision control and accurate measurement of the reaction processes. In large pores, such flow is often described by invasion percolation models that are essentially hydrodynamic [6, 7]. For mesopores, due to the small pore size and the short t_s , which is at the ps- μ s level, the capillary effect and the probabilistic characteristic in the filling process are important [8, 9].

Over years, a number of studies have been carried out on the diffusion of liquid molecules in the nanoenvironment.

Through nuclear magnetic resonance (NMR) analysis, it has been confirmed that there exists an interface layer near the solid-liquid interface, where surface diffusion is dominant [10, 11]. The average molecular diffusion distance can be described by

$$\langle x^2 \rangle = \tilde{\alpha}t + \tilde{\beta}t^\kappa \quad (1)$$

where t is time and $\tilde{\alpha}$, $\tilde{\beta}$ and κ are system parameters [12]. The first term in the RHS captures the single-file diffusion in the interior (normal flow) and the second term reflects the surface diffusion (subdiffusive or superdiffusive flow). However, currently the studies on the confined inflow subjected to a dynamic pressure are rare. In order to relate the liquid behavior in the nanoporous particle to the processing parameters, in this paper we will develop a model based on the equilibrium of cluster number density. The phenomenological probability functions will be used to capture the randomness of the pore cluster nucleation in the nanoenvironment and the flow rate will be assessed by a dimensional analysis.

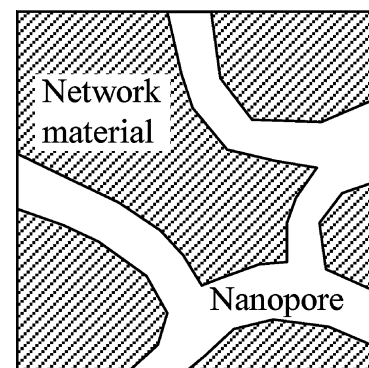


Fig. 1. The mesoporous structure.

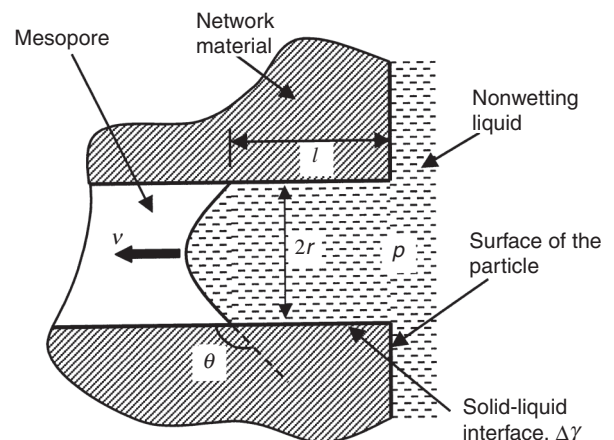


Fig. 2. The nonwetting flow confined in a mesopore under the external pressure, p .

*Email: yqiao@uakron.edu

2. Confined Non-Wetting Inflow in a Single Mesoporous Particle

Borman *et al.* [13, 14] modeled the flow in porous media as a process consisting of nucleation and growth of clusters of filled pores. Under a relatively low pressure the solid and the liquid are separate, while as the pressure increases to above p_{cr} , the filled status becomes energetically favorable. Thus, starting from the particle surface, the liquid is forced to penetrate into the porous structure at a number of points and flow in adjacent pores, forming filled pore clusters and eventually resulting in saturation. Note that in the following discussion the pressure difference is assumed to be sufficiently high such that the factor of the pore size comes in by affecting the inflow rate instead of determining whether or not the capillary effect can be overcome.

To describe this phenomenon quantitatively, the concept of the number density of filled mesopore clusters (FMC), $n(c, \varphi, t)$, can be employed. $n(c, \varphi, t)$ is defined as the number of FMC with depth c and angle φ at time t . Once $p > p_{cr}$ and the inflow occurs, the liquid randomly penetrates into the particle surface. The filled clusters expand along both radial and tangential directions. In this framework, the average behavior of the inflow can be considered as a continuous process of nucleation of new FMCs on the particle surface and the growth and coalescence of existing FMCs in the interior (see Fig. 3).

Consider the phase space of n spanned by c and φ . In a small time increment Δt , the change of the number of FMCs in the area of c to $c + \Delta c$ and φ to $\varphi + \Delta\varphi$ can be stated as

$$\Delta n = \Delta t \{ n_N + [\bar{C}(c)\bar{n}(c) - \bar{C}(c + \Delta c)\bar{n}(c + \Delta c)] + [\bar{\Psi}(\varphi)\bar{n}(\varphi) - \bar{\Psi}(\varphi + \Delta\varphi)\bar{n}(\varphi + \Delta\varphi)] \} \quad (2)$$

where n_N is the nucleation rate, \bar{C} is the average radial growth rate, $\bar{\Psi}$ is the average tangential growth rate, and \bar{n} is the average number density. If we neglect the high-order terms, as $\Delta t, \Delta c$ and $\Delta\varphi \rightarrow 0$, Eq. (2) can be rewritten as

$$\frac{\partial n(c, \varphi, t)}{\partial t} + \frac{\partial [C(c, t)n(c, \varphi, t)]}{\partial c} + \frac{\partial [\Psi(\varphi, t)n(c, \varphi, t)]}{\partial \varphi} = n_N(c, \varphi, t) \quad (3)$$

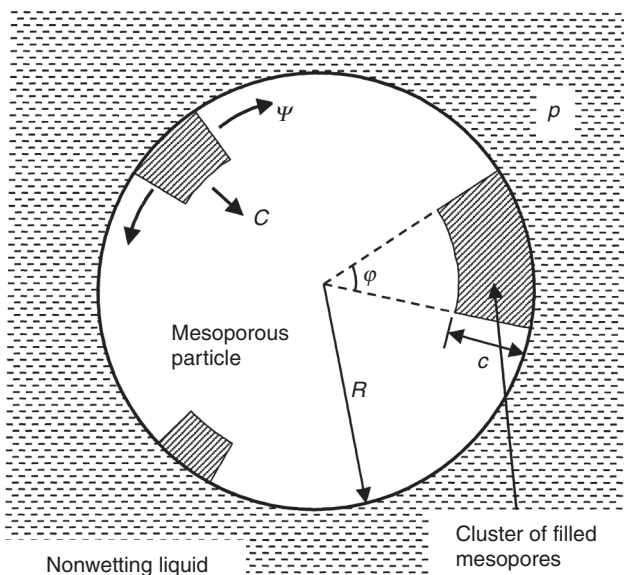


Fig. 3. Schematic diagram of the growth of filled mesopore clusters.

where C and Ψ are the radial growth rate and the tangential growth rates of FMC, respectively. Equation (3) describes the equilibrium of FMC number density. The second and third terms at LHS capture the effect of FMC growth, and the RHS reflects the nucleation and coalescence. When the total FMC volume equals the particle volume, i.e.

$$\iint n(c, \varphi, t_s) \cdot \lambda \cdot \left(1 - \cos \frac{\varphi}{2}\right) \times (3R^2 + c^2 - 3cR) d\varphi dc = \frac{4}{3}\pi R^3 \quad (4)$$

where R is the particle radius and λ is a geometry factor, the particle is saturated. For isotropic FMC growth, $\lambda = 2\pi/3$.

The flow rate v in a mesopore should be related to the external pressure p , the liquid density ρ , the viscosity μ , the pore radius r , and the interfacial tension γ . Similar with Eq. (1), the inflow rate can be decomposed into two components

$$v = f_1(p, \rho, \gamma, \mu) + f_2(p, \rho, r, \mu) \quad (5)$$

where f_1 and f_2 reflect the interface flow and the normal flow in the interior, respectively. Note that the interface flow is independent of pore size r and the normal flow in the interior is independent of γ . Based on the Π theorem [15] and following Eq. (1), the average inflow rate can be described by a two-power-law function

$$v = \alpha'' \frac{pr}{\mu} \left(\frac{p\rho r^2}{\mu^2}\right)^{\beta'} + \alpha' \sqrt{\frac{p}{\rho}} \left(\frac{p\mu^2}{\rho\gamma^2}\right)^{\beta} \quad (6)$$

where α'', α', β , and β' are system parameters. According to the classic circular Poiseuille flow solution, for normal flow $v \propto p$, i.e. $\beta' = 0$. The parameters α'' and α' indicate the degree of importance of the interface layer and can be assumed to be proportional to the cross-sectional areas. Hence, $\alpha'' \propto (1 - d_0/r)^2$ and $\alpha' \propto 1 - [(r - d_0)/r]^2$, with d_0 being the thickness of the interface layer. Note that when $d_0 \rightarrow 0$ or $r \rightarrow \infty$ Eq. (6) should converge to the result of conventional fluid mechanics. Consequently, the inflow rate can be obtained as

$$v = \left(1 - \frac{d_0}{r}\right)^2 \frac{pr}{8\mu\bar{L}} + \alpha \left[1 - \left(\frac{r - d_0}{r}\right)^2\right] \sqrt{\frac{p}{\rho}} \left(\frac{\rho\gamma^2}{p\mu^2}\right)^{\beta} \quad (7)$$

where \bar{L} is the effective pore aspect ratio and α is a material constant [16]. Since v increases with p and γ and decreases with ρ and μ , the value of β should be in the range of 0 to 1/2.

The average radial growth rate of FMC can then be calculated as

$$C = \int_0^\infty P(r)v dr \quad (8)$$

where $P(r)$ is the pore size distribution. Similarly, the average tangential growth rate is

$$\Psi = \frac{2}{R - c/2} \int_0^\infty P(r)v dr. \quad (9)$$

At the small time scale, the invasion of the nonwetting liquid cannot be considered as an equilibrium process [1, 8, 9]. At time t , the number of pores in the particle surface where the inflow starts can be stated as

$$\hat{n}_N(c, \varphi, t) = \eta_0 P\left(\frac{\varphi R}{2}\right)_{c=\frac{c}{\Psi}\varphi} \times \left[1 - \frac{1}{4\pi R^2} \iint n(c, \varphi, t) \cdot \zeta \varphi R^2 dc d\varphi\right]. \quad (10)$$

The term in the bracket indicates the fraction of the surface area of empty pores, with ζ being a geometry factor, which equals π when the FMCs are small. The parameter $\eta_0 = \eta_1 \int_0^{r_{cr}} P(r) dr$, with η_1 being a constant, $r_{cr} = 2\gamma_1 \cos \theta / p$ being the lower limit of the size of the filled pores, γ_1 being the surface tension of the non-wetting liquid, and θ being the contact angle.

The probability for the center-to-center distance between two adjacent FMCs to be x is [17]

$$f(\hat{x}) = \sqrt{D_0}(1 - \hat{x})^{\sqrt{D_0}-1} \quad (11)$$

with $\hat{x} = x/2\pi R$ and $D_0(t) = \iint n(c, \varphi, t) dc d\varphi$ being the total number of FMC. Hence, the probability of coalescence is

$$g(x, t) = \eta \cdot f(\hat{x}) \int_0^x n_c(\varphi, t) \left[1 - \int_0^{x/R-\varphi} n_c(\tilde{\varphi}, t) d\tilde{\varphi} \right] d\varphi \quad (12)$$

where η is the normalization coefficient and $n_c(\varphi, t) = (1/D_0) \int_0^R n(c, \varphi, t) dc$. Note that the probability nature of the inflow process is related to the pore size distribution as well as the secondary factors affecting the capillary effect such as the precursor film formation and the dependence of the contact angle on flow direction.

The nucleation rate due to the FMC coalescence can then be obtained as

$$\tilde{n}_N(c, \varphi, t) = D_0(t) [\tilde{g}(\varphi, t) - 2\hat{g}(\varphi, t)]_{c=\frac{\varphi}{2R}} \quad (13)$$

where

$$\begin{aligned} \tilde{g}(\varphi, t) &= 2 \int_0^{\varphi R} g(x) \\ &\times \left\{ \int_0^{(\varphi R-x)/2} n_c(\tilde{c}, t) \left[1 - \int_0^{\varphi R-x-\tilde{c}} n_c(\hat{c}, t) d\hat{c} \right] d\tilde{c} \right\} dx \end{aligned}$$

is the distribution of a FMC nucleated from two smaller FMC with the size distribution of

$$\hat{g}(\varphi, t) = \int_0^{\pi R} g(x) \frac{n_c(\varphi, t)}{\int_0^{x/2R} n_c(\varphi, t) d\varphi} dx.$$

Finally, the overall nucleation rate can be obtained as $n_N = \tilde{n}_N + \hat{n}_N$, and the boundary condition and initial condition should be $n(0, 0, t) = 0$ and $n(c, \varphi, 0) = 0$, respectively. The model for the kinetics of confined inflow is now complete.

3. Discussion and Conclusions

Figure 4 shows the numerical results of the evolution of n_c under $p = 0.1$ MPa in a particle with a radius of 100 μm . The surface tension and the contact angle are taken as 72 mJ/m^2 and 120°, respectively. The pore size distribution is described by a lognormal function with a mean value \bar{r} of 10 nm and a standard deviation σ of 3 nm. The characteristic time $t^* = 1 \mu\text{s}$. Based on the NMR data, the value of β is taken as 1.2 and d_0 is assumed to be 5 nm [10, 11]. The value of η_1 can be somewhat arbitrarily chosen since it depends on the time resolution and has little influence on the absolute value of n_c . In this paper it is set to 10^{-3} . The viscosity and density of the liquid are taken as 10^{-3} Pa·s and 10^3 kg/m^3 , respectively.

It can be seen that at the early stage when \hat{n}_N is dominant the peak of n_c distribution is around \bar{r} . With the growth of FMCs the peak moves toward the higher end and the height starts to decrease due to the size dependence of Ψ . As the number of FMCs becomes larger, the coalescence of adjacent FMCs is increasingly pronounced and the distribution curve consists of two plateau

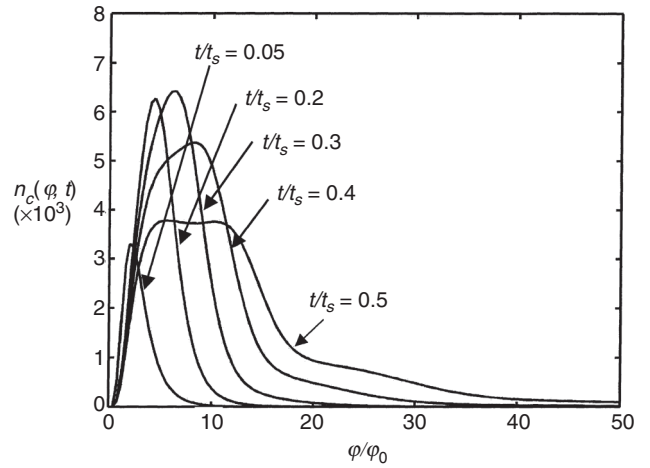


Fig. 4. Evolution of $n_c(\varphi, t)$, where $\varphi_0 = 2r/R$ is the characteristic angle.

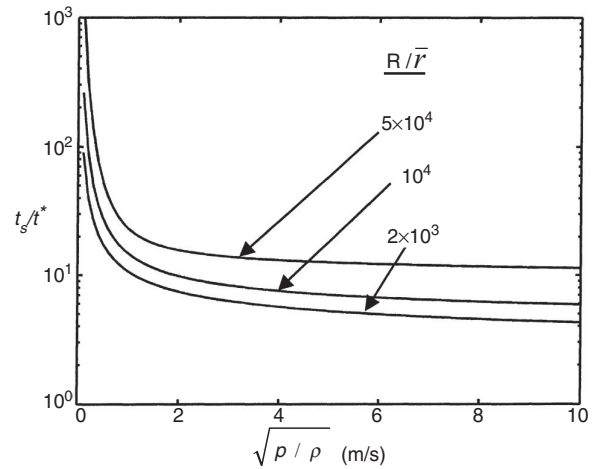


Fig. 5. The saturation time as function of $p\mu^2/\rho\gamma^2$ and R/\bar{r} .

regions caused by the decrease in n_c in the lower φ range and the rapid increase in the higher φ range, respectively. The two regions are separated by a sharp drop in n_c associated with the tangential growth. Eventually the plateau at lower φ range vanishes and when saturation is reached the total FMC number is reduced to 1.

The saturation time, t_s , is influenced by a number of factors. The numerical results shown in Fig. 5 indicate that t_s decreases with increasing p and \bar{r} or decreasing R , as it should. The value of t_s tends to infinity as $p \rightarrow 0$, and decreases rapidly until $\sqrt{p/\rho}$ exceeds 1, after which t_s becomes relatively insensitive to the change in p . Through Eqs. (10) and (13), it can be seen that the t_s - R relation is highly nonlinear. As the particle radius increases the probability of FMC coalescence is lowered and thus the filling process is prolonged, which is equivalent to reducing the pore size \bar{r} . Therefore, even if the filling rate v were independent of r the inflow in the mesoporous particle is still not scalable. This mechanism, together with the size effect of v , results in the nonlinear t_s - σ relationship.

In a dynamic environment, the characteristic time of pressure variation, p/\dot{p} , is comparable to the saturation time. Under this condition, the pressure p cannot be assumed to be a constant. By replacing p by $\dot{p}t$ in Eqs. (3)–(15), this effect can be studied numerically and the results are shown in Fig. 6. As \dot{p} rises, the acceleration of inflow becomes higher and thus t_s is lowered. The \dot{p} dependence of t_s is somewhat stronger than that of p , since, due to the relatively low early pressure, the early stage of FMC

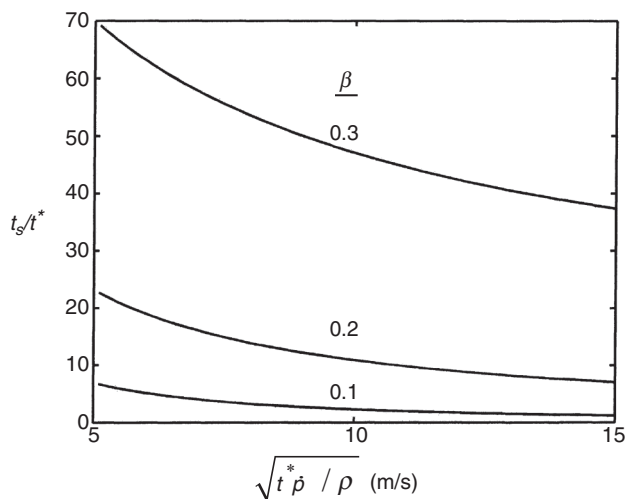


Fig. 6. The saturation time as function of $t^* p_0 / \rho$ and β .

evolution where the FMC growth is nearly isolated is prolonged. In Fig. 6, we also show the influence of β . As suggested by Eq. (7), increasing β has a beneficial effect in increasing the saturation time. The large extent of variation of t_s associated with the change in β indicates clearly that the interface layer plays an important role in the absorption process.

To summarize, in this paper, based on the analysis of FMC number density, a framework has been developed for the kinetics of the non-wetting flow in a mesoporous particle. The process is modeled as the nucleation, growth, and coalescence of filled pore clusters, with the fractal nature of the inflow being neglected. The following conclusions are drawn: (1) the evolution of n_c can be characterized by the shifting and eventual vanishing of the plateau in the small angle region and the development of

the secondary plateau in the large angle region; (2) a number of factors, such as the pore size distribution, the particle size, the external pressure, come in by affecting both the inflow rate and the coalescence processes; and (3) the influence of the interface layer is significant.

Acknowledgement

This work has recently been supported by the ARO under Grant W911NF-04-1-0244, for which we are grateful to Dr. David M. Stepp. Special thanks are also due to the reviewer of this article for the valuable suggestions.

References

1. Polartz, S. and Smarsly, B., *J. Nanosci. Nanotech.* **2**, 581 (2002).
2. Yang, C. M. and Chao, K. J., *J. Cn. Chem. Soc.* **49**, 883 (2002).
3. Raman, N. K., Anderson, M. T. and Brinker, C. H., *Chem. Mater.* **8**, 1682 (1996).
4. Evans, D. F. and Wennerstrom, H., "The colloidal domain", (Wiley-VCH, NY 1999).
5. Terasaki, O. T. *et al.*, *Studies Surface Sci. Catalysis* **141**, 27 (2001).
6. Dommermich, D. G. and Yue, D. K. P., *J. Fluid Mech.* **178**, 195 (1987).
7. Blunt, M. J., *Curr. Opin. Colloid In.* **6**, 197 (2001).
8. Dabrowski, A., *Adv. Colloid Interface Sci.* **93**, 135 (2001).
9. Pandey, P. and Chauhan, R. S., *Prog. Polym. Sci.* **26**, 853 (2001).
10. Cramer, C., Cramer, T., Kremer, F. and Stannarius, R., *J. Chem. Phys.* **106**, 3730 (1997).
11. Yi, J. and Jonas, J., *J. Phys. Chem.* **100**, 16789 (1996).
12. Metzler, R. and Klafter, J., *Phys. Rep.* **339**, 1 (2000).
13. Borman, V. D., Belogorlov, A. A., Grekhov, A. M., Tronin, V. N. and Troyan, V. I., *JETP Lett.* **74**, 287 (2001).
14. Borman, V. D., Grekhov, A. M. and Troyan, V. I., *J. Exp. Theo. Phys.* **91**, 170 (2000).
15. Szirtes, T., "Applied Dimensional Analysis and Modeling", (McGraw-Hill, New York, 1997).
16. Liu, D., Wijeratne, S. and Litster, J. D., *Scand. J. Metall.* **26**, 79 (1997).
17. Chen, H. and Qiao, Y., *J. Appl. Math. Mech.*, to be published.